Transmission of 2 bits/symbol over RoF and RoFSO links with different architectures for ubiquitous coverage

Dong-Nhat Nguyen
Department of Electromagnetic Field
Czech Technical University in Prague
Prague, Czech Republic
dongnhat@fel.cvut.cz

Luis Vallejo
Instituto de Telecomunicaciones y Aplicaciones Multimedia, ITEAM
Universitat Politècnica de València
Valencia, Spain
luivalc2@iteam.upv.es

Jan Bohata
Department of Electromagnetic Field
Czech Technical University in Prague
Prague, Czech Republic
bohatja2@fel.cvut.cz

Stanislav Zvanovec
Department of Electromagnetic Field
Czech Technical University in Prague
Prague, Czech Republic
xzvanove@fel.cvut.cz

Beatriz Ortega
Instituto de Telecomunicaciones y Aplicaciones Multimedia, ITEAM
Universitat Politècnica de València
Valencia, Spain
bortega@dcom.upv.es

Zabih Ghassemlooy
Faculty of Engineering and Environment
Northumbria University
Newcastle upon Tyne, United Kingdom
z.ghassemlooy@northumbria.ac.uk

***Abstract*—This paper investigates integrated radio-over-fiber and radio-over-free-space optic links in a passive optical network architecture for ubiquitous wireless coverage. Two optical millimeter-wave generation techniques, namely optical heterodyning and optical modulator-based up-conversion are used. In the first configuration, simulation results are achieved for transmission of 20-40 Gb/s 4-PAM over the 60 GHz heterodyned hybrid link. In the second configuration, transmission of 20 MHz 4-QAM over the up-converted 25 GHz hybrid system is examined. System performance evaluation and practical feasibility is carried out in terms of the received optical powers, bit error rates, eye diagrams, error vector magnitude and constellation diagrams.**

Keywords—radio-over-fiber, free-space optics, passive optical networks, turbulence, millimeter-wave

I. INTRODUCTION

Current mobile networks deploy a large number of traditional tower-mounted macro base stations (BSs) where each BS covers a cell, processes and transmits its own signal. However, it is difficult to provide wide coverage to rural areas and underserved communities using these traditional BSs due to the high cost of installation and maintenance. Future mobile networks need to fulfil this demand apart from the higher data rates R_d and lower transmission latency. The cloud radio access network (C-RAN) with dense deployment of small-cell BSs (i.e., much smaller coverage over the traditional macro-cell BS) as a cost-effective architecture has attracted great interest from both the research community and the commercial sector over the past decade [1], [2]. C-RAN is considered as a typical realization of a mobile network supporting soft and green technologies in the future mobile networks since most of the signal processing, signal generation and modulation functions can be implemented at a central station (CS). This helps to simplify the antenna sites at the BSs with the remote radio head architecture. For that reason, C-RAN based on a radio-over-fiber (RoF) fronthaul link is highly applicable for small-cell and ultra-dense small-cell networks. Note that, RoF operating in the high radio frequency (RF) bands, such as in the millimeter wave (mmW) [3] and even terahertz-wave [4] have also recently gained tremendous attention for applications in 5th generation (5G) mobile networks and beyond. The mmW signal can be optically generated by different techniques, although optical modulator-based up-conversion [5] and optical heterodyning [6] are the most well-known and widely used in the literature.

It is worth to mention that, the installation of optical fiber (OF) cables between the CS and BS within the RoF-based C-RAN architecture can be challenging and costly. The use of OF cables is also impractical in many cases considering the geographical constraints and physical obstacles. The free-space optical (FSO) communication-based technology [7] could be therefore adopted to solve the aforementioned issues to maintain the seamless connectivity as a backup or a last-mile access link since the FSO technology offers unique features such as large bandwidth, license-free spectrum, high bit rate, easy and quick deployment. FSO transceivers operating at a wavelength of 1550 nm, which is compatible with the 3rd transmission window in OF communications (OFC), and R_d of up to 30 Gb/s over a transmission distance L of 1.5 km are commercially available [8]. Radio-over-FSO (RoFSO), therefore, has also been introduced and demonstrated since 2006 [9], where researchers from the University of Oklahoma, USA, transported the modulated analog RF signals within the range of 46 to 870 MHz over an indoor 3 m FSO link and characterized the key performance parameters (i.e., carrier-to-noise ratio and spurious free dynamic range) without considering the effects of atmospheric phenomena such as turbulence. The turbulence strength is usually evaluated by the refractive index structure parameter C_n^2 ($\mathrm{m}^{-2/3}$) [7]. C_n^2 can vary from 10^{-17} up to 10^{-12} $\mathrm{m}^{-2/3}$ for weak-to-strong turbulence regimes, respectively. It is well-known that FSO links are affected by

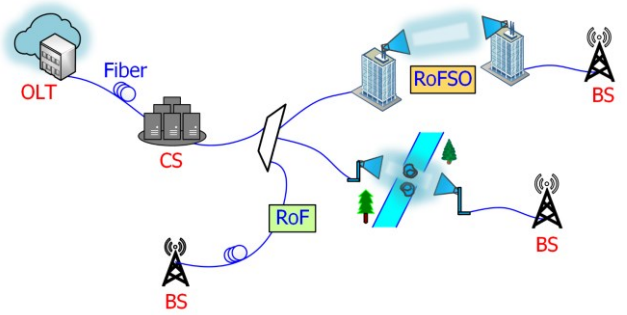

Figure 1. The simplified concept of delivering RF signal over hybrid RoF-FSO systems to remote areas in PON architecture.

turbulence strength, which may reduce the quality-of-service. Then, in 2009, researchers from Waseda University, Japan carried out a complete and long-term RoFSO measurements with RF ranging from 450 kHz to 420 MHz and a FSO link span of 1 km [10]. The link was demonstrated in an outdoor environment and the effect of turbulence was therefore comprehended. Seamless integration of RoF and RoFSO (i.e., RoF-FSO) operating in the mmW region are thus very attractive to deliver wide coverage in rural areas [11], [12]. We recently proposed and successfully demonstrated a 25 GHz mmW link with 4/16/64-quadrature amplitude modulation (QAM) over an integrated RoF-FSO link with the FSO path being exposed to weak-to-strong turbulence regimes [13].

In this work, we propose and investigate the transmission of 2 bits/symbol using 4-level pulse amplitude modulation (4-PAM) and 4-QAM over the seamless RoF-FSO in a passive optical network (PON) architecture to further scale the system mobility and reduce the cost for ubiquitous coverage, see Fig. 1. Note that, there are a number of benefits such as energy savings, scalability, signal security and higher split ratio that make PON the main and most extensively employed network in OFC systems. In addition, both 4-PAM and 4-QAM have been evaluated as promising candidates for the next-generation PON [14], [15]. Regarding the optical mmW generation, two different schemes are considered at the CS in this work as follows:

1) Scheme A: Transmission of 4-PAM over a 60 GHz hybrid link using optical heterodyning.
2) Scheme B: Transmisison of 4-QAM over a 25 GHz hybrid link using optical Mach-Zehnder modulator (MZM)-based up-conversion.

Both frequencies are considered in 5G mobile networks [16]. Another goal of this work is also to evaluate the effect of both uniform and non-uniform turbulence on the FSO link and therefore the hybrid system performance.

The remaining part of the paper is structured as follows. Section II describes the simulation setup and results of Scheme A. Section III presents the experimental setup and results of Scheme B. Finally, the conclusion is given in Section IV.

II. Simulation Setup and Results Using 4-PAM with 60 GHz MMW Carrier Frequency of 60 GHz (Scheme A)

A. Simulation Setup

Fig. 2 shows the simulation setup of 4-PAM transmission over the implemented system using the optical heterodyning technique for mmW signal generation. Note that, an experimental demonstration of this scheme has been carried out in [17], but only investigating transmission from OLT to CS to BS (ODN not included) and using low spectral efficiency non-return-to-zero signal.

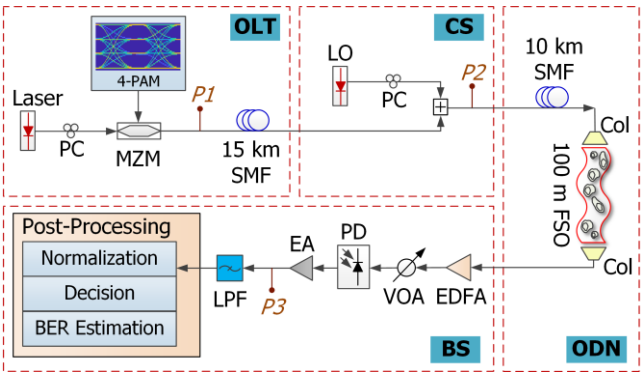

Figure 2. Simulation setup (Scheme A).

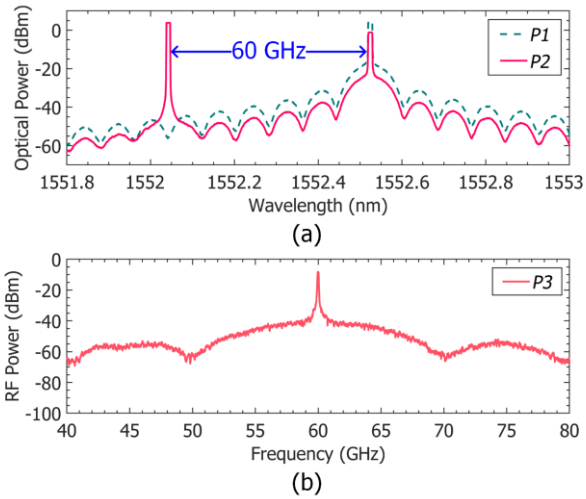

Figure 3. (a) Optical and (b) electrical spectra obtained at respective locations (*P*1, *P*2, *P*3 – see the setup in Fig. 2).

At the optical line terminal (OLT), an optical signal emitted by a distributed feedback (DFB) laser is applied through a polarization controller (PC) into a MZM, where it is externally modulated by an electrical 4-PAM signal at 20 Gb/s. The optical baseband signal is then transmitted over a 15 km standard single-mode fiber (SMF) representing a typical optical link. Optical heterodyning approach to generate an mmW signal at the CS is based on the combination of the optical baseband signal with another DFB laser (i.e., a local oscillator (LO) laser) which is set to a lasing frequency exactly 60 GHz apart from the former one. The corresponding spectra at different positions in Scheme A are indicated in Fig. 3. The optical mmW signal is further transmitted over the optical distribution network (ODN), which consists of 10 km SMF and 100 m FSO channel with weak uniform turbulence C_n^2 of 1.3×10^{-16} $\mathrm{m}^{-2/3}$. Note that, the employed FSO collimators (Col) parameters are

based on commercial devices [8]. The optical signal is then amplified by using an erbium-doped fiber amplifier (EDFA) and then directly detected by a PIN photodiode (PD), which has a responsivity of 0.6 A/W and a dark current of 10 nA, for opto-electronic conversion at the BS. A variable optical attenuator (VOA) is used to adjust the received optical power P_r at the the PD. The recovered electrical signal is then amplified by a low-noise electrical amplifier (EA), which has a 30 dB gain, followed by a low-pass Bessel filter (LPF). Finally, the signal is post-processed in MATLAB-based digital signal processing module to carry out normalization, symbol decision and bit error rate (BER) estimation. The main parameters adopted in the simulation are summarized in Table 1.

Table 1. Main simulation parameters (Scheme A).

Parameter	Value
Laser 1	
• Wavelength	1552.524 nm
• Output power	16 dBm
Laser 2 (LO)	
• Wavelength	1552.042 nm
• Output power	6.8 dBm
Modulation format	4-PAM
mmW carrier frequency	60 GHz
SMF	
• Length in OLT	15 km
• Length in ODN	10 km
• Dispersion	17 ps/(nm·km)
FSO	
• Aperture diameter	10 cm
• Length	100 m
EDFA	
• Output power	1 dBm
• Noise figure	3 dB

B. Simulation Results

To investigate the maximal allowable transmission capacity of the hybrid link (Scheme A) when delivering 4-PAM, we show the BER versus the R_d of the received 4-PAM signal over the hybrid transmission link at P_r of 1 dBm – see Fig. 4. As expected, the BER increases with the R_d, where a maximum R_d of about 30 Gb/s can be achieved at the forward error correction (FEC) BER limit of 3.8×10^{-3}.

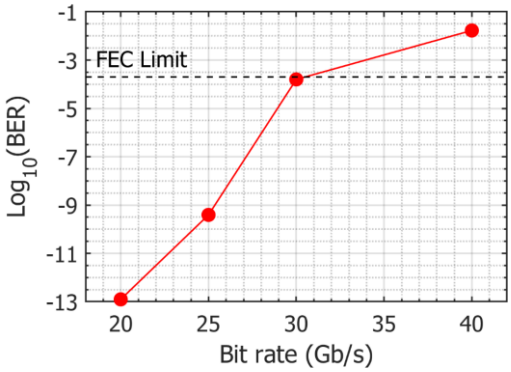

Figure 4. BER of 4-PAM signal after hybrid transmision at different bit rates obtained at P_r of 1 dBm and C_n^2 of 1.3×10^{-16} $m^{-2/3}$.

A set of the corresponding received 4-PAM eye diagrams at R_d of 20, 25, 30 and 40 Gb/s obtained at P_r of 1 dBm is shown in Figs. 5 (a)-(d), respectively. As R_d increases, the eye diagrams accumulate more intersymbol interference, which has an impact on the corresponding BER as depicted in Fig. 4.

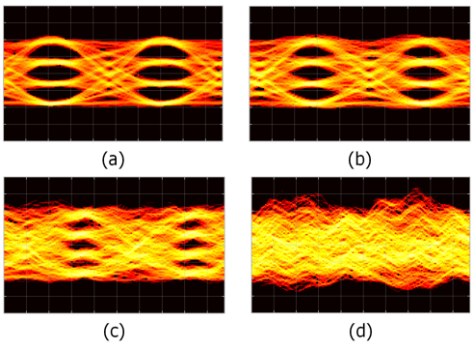

Figure 5. Eye diagrams of 4-PAM signal after transmission captured at P_r of 1 dBm with a data rate of (a) 20 Gb/s, (b) 25 Gb/s, (c) 30 Gb/s and (d) 40 Gb/s.

To further study the performance of 20 Gb/s 4-PAM under the effect of turbulence over a 100 m FSO channel for the proposed hybrid link, we consider both uniform and non-uniform turbulence scenarios as can be seen in Fig. 6. In detail, for the former, we set C_n^2 of 2.0×10^{-15} $m^{-2/3}$ along a 100 m FSO link to mimic the moderate uniform turbulence. For the latter, we have considered a strong turbulence (i.e., C_n^2 of 1.6×10^{-13} $m^{-2/3}$) at the center of the FSO link (i.e., 40 m) and weak turbulence (i.e., C_n^2 of 1.3×10^{-16} $m^{-2/3}$) for both ends of the channel in order to create a non-uniform turbulence which the link may experience in real practical outdoor environments.

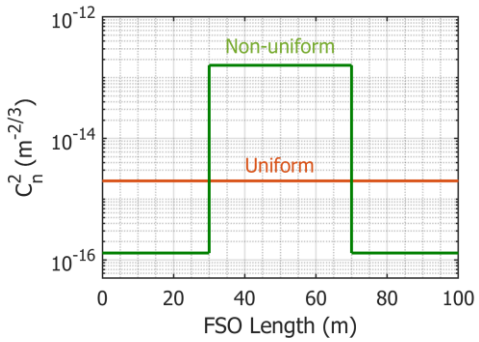

Figure 6. Turbulence scenarios considered in the simulation.

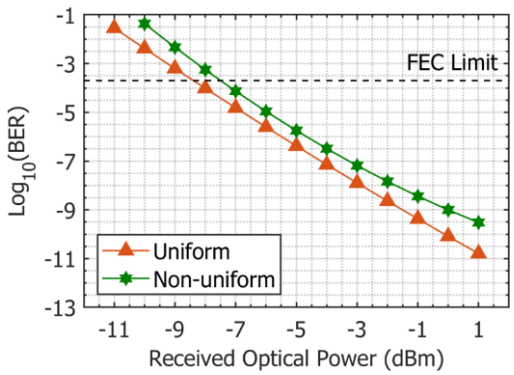

Figure 7. BER versus P_r for 4-PAM transmisison at 20 Gb/s with different turbulence scenarios.

Fig. 7 compares the simulated BERs as a function of P_r for the two considered turbulence scenarios. The BER is, in both cases, well below the FEC limit for P_r larger than -7 dBm. As can be clearly seen, at the FEC BER limit there is 1 dB power penaty for the link with non-uniform turbulence compared with the channel with uniform turbulence. Compared to weak uniform turbulence – C_n^2 of 1.3×10^{-16} $m^{-2/3}$ as shown in Fig. 4, moderate uniform turbulence with C_n^2 of 2×10^{-15} $m^{-2/3}$ and non-uniform turbulence result in more than two and three orders of magnitude degradation in BER.

III. Experimental Setup and Results Using 4-QAM Signal with MMW Carrier Frequency of 25 GHz (Scheme B)

A. Experimental Setup

The experimental setup of a hybrid RoF-FSO link using 4-QAM with optical MZM-based up-conversion technique is shown in Fig. 8. At the OLT, the optical signal from the laser (ID Photonics CoBrite-DX4) is externally modulated by 4-QAM with an intermediate frequency of 200 MHz, generated by a vector signal generator (R&S SMW 200A) and then transmitted over a 15 km of SMF. Unlike Scheme A, which uses optical heterodyning at the CS, in the Scheme B, another MZM (MZM 2) is used for up-conversion. MZM 2 is externally modulated by 12.5 GHz RF clock from a signal generator (R&S SMF 100A). Note that, it is biased at the minimum transmission point, and therefore the optical spectrum with suppressed carrier at the output of MZM 2 and the frequency spacing of 25 GHz between two sidebands are achieved, see Fig. 9. The carrier suppression ratio of about 23 dB is obtained. The optically amplified signal is then transmitted over ODN, which consists of 10 km SMF and 2 m FSO channel within an indoor atmospheric chamber.

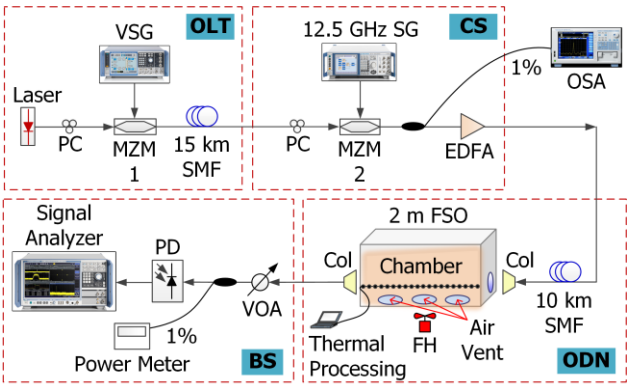

Figure 8. Experimental setup (Scheme B).

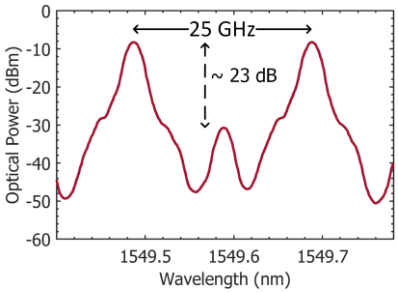

Figure 9. Optical spectrum featuring double-sideband with optical carrier suppression measured at the MZM 2 output.

Non-uniform turbulence is generated using a fan heater (FH), which blows hot air to the middle of chamber via the central air vent. To accurately measure the thermal profiles and then determine C_n^2, 20 thermal sensors are used, see measurements in Fig. 10. More detail on C_n^2 measurements within the chamber can be found in [13]. At the BS, the optical signal is detected using a high-speed PD, the output of which evaluated using a signal analyzer. The key experimental parameters are summarized in Table 2.

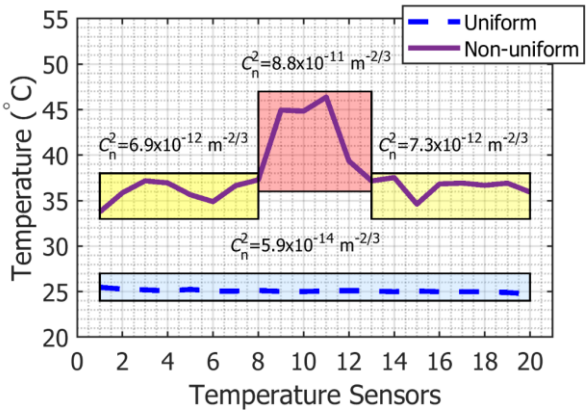

Figure 10. Turbulence scenarios considered in the experiment.

Table 2. Main experimental parameters (Scheme B).

Parameter	Value
Laser	
• Wavelength	1549.6 nm
• Output power	16 dBm
Modulation format	4-QAM
mmW carrier frequency	25 GHz
SMF	
• Length in OLT	15 km
• Length in ODN	10 km
• Dispersion	17 ps/(nm·km)
FSO	
• Aperture diameter	2.54 cm
• Length	2 m
EDFA	
• Output power	6 dBm
• Noise figure	< 4 dB

B. Experimental Results

Fig. 11 shows the measured error vector magnitude (EVM) as a function of P_r for 20 MHz 4-QAM following transmission over the hybrid link (Scheme B) for different turbulence scenarios. Also shown is the 18.5% EVM required limit for 4-QAM according to the third-generation partnership project (3GPP) specifications [18].

Apparently, at P_r of 6 dBm, the EVMs of 4-QAM under uniform and non-uniform turbulences are 9.5 and 13%, respectively, which leads to an EVM degradation of 3.5%. Both EVM values, however, are well below EVM requirements. The results also indicate less than 1 dB optical power degradation at the EVM limit of 18.5% due to the influence of non-uniform turbulence in the FSO channel.

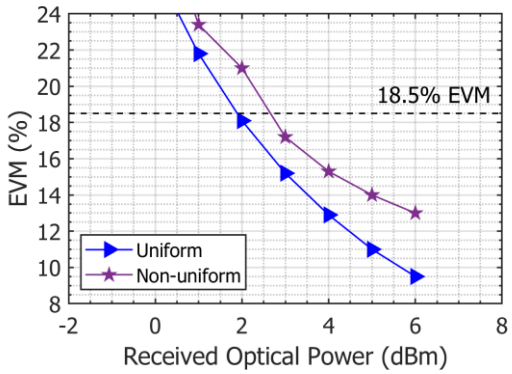

Figure 11. EVM versus P_r for 20 MHz 4-QAM transmisison with different C_n^2.

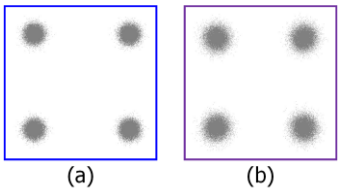

Figure 12. Constellation diagrams captured at P_r of 6 dBm of 20 MHz 4-QAM signal after tranmission under (a) uniform and (b) non-uniform turbulence, respectively.

To further demonstrate the effect of uniform and non-uniform turbulence on the signal quality, we show in Fig. 12 the measured constellation diagrams of the received 4-QAM measured at P_r of 6 dBm. Under non-uniform turbulence, Fig. 12(b), the 4-QAM symbol size is more diffused in comparison to the constellation under uniform turbulence shown in Fig. 12(a). This corresponds to simulation results as presented in Section II.

IV. Conclusions

We analyzed two different hybrid RoF-FSO transmission links based on optical heterodyning and optical modulator-based up-conversion techniques for ubiquitous broadband wireless access. Two bits/symbol signals namely 4-PAM and 4-QAM were transmitted over the proposed systems. The impact of FSO channel under the effect of turbulence is also examined in detail. At the maximum P_r, for the simulation results with 20 Gb/s 4-PAM, the effect of non-uniform turbulence caused more than one order of magnitude degradation in BER compared to uniform turbulence. While for 20 MHz 4-QAM transmission in experiment, the EVM penalty beween non- and uniform turbulence is about 3.5%. Both experimental and simulation results therefore showed good agreement regarding the impact of non-uniform turbulence, which is more severe in comparison to the uniform turbulence on the system performance.

Acknowledgment

This work is supported by International Mobility of Researchers in CTU (CZ.02.2.69/0.0/0.0/16_027/0008465) and MEYS INTER-COST project (within LTC18008).

References

[1] China Mobile Reserach Institute, "C-RAN: the road towards green RAN, white paper," 2011.

[2] I. A. Alimi, A. L. Teixeira, and P. P. Monteiro, "Toward an efficient C-RAN optical fronthaul for the future networks: A tutorial on technologies, requirements, challenges, and solutions," *IEEE Commun. Surv. Tutorials*, vol. 20, no. 1, pp. 708–769, 2018.

[3] P. T. Dat, A. Kanno, and N. Yamamoto, "Seamless convergence of fiber and wireless systems for 5G and beyond networks," *J. Lightwave Technol.*, vol. 37, no. 2, pp. 592–605, 2019.

[4] T. Kawanishi, "THz and photonic seamless communications," *J. Lightwave Technol.*, vol. 37, no. 7, pp. 1671–1679, 2019.

[5] L. Vallejo *et al.*, "Impact of thermal-induced turbulent distribution along FSO link on transmission of photonically generated mmW signals in the frequency range 26–40 GHz," *IEEE Photonics J.*, vol. 12, no. 1, pp. 1–9, Feb. 2020.

[6] E. Martin *et al.*, "28 GHz 5G radio over fibre using UF-OFDM with optical heterodyning," in *International Topical Meeting on Microwave Photonics (MWP)*, 2017, p. Th2.4.

[7] Z. Ghassemlooy, W. O. Popoola, and S. Rajbhandari, *Optical wireless communications – system and channel modelling with Matlab*, 2nd ed. Cham: CRC Press, 2019.

[8] "30 Gbit/s ARTOLINK." [Online]. Available: http://artolink.com/.

[9] H. H. Refai, J. J. Sluss, Jr., and H. H. Refai, "Comparative study of the performance of analog fiber optic links versus free-space optical links," *Opt. Eng.*, vol. 45, no. 2, p. 025003, Feb. 2006.

[10] P. T. Dat *et al.*, "Studies on characterizing the transmission of RF signals over a turbulent FSO link," *Opt. Express*, vol. 17, no. 10, p. 7731, 2009.

[11] P. T. Dat, A. Kanno, K. Inagaki, T. Umezawa, N. Yamamoto, and T. Kawanishi, "Hybrid optical wireless-mmWave: ultra high-speed indoor communications for beyond 5G," in *IEEE INFOCOM 2019 - IEEE Conference on Computer Communications Workshops (INFOCOM WKSHPS)*, 2019, pp. 1003–1004.

[12] Y. Alfadhli *et al.*, "Real-time FPGA demonstration of hybrid bi-directional MMW and FSO fronthaul architecture," in *2019 Optical Fiber Communications Conference and Exhibition, OFC 2019 - Proceedings*, 2019, p. W2A.39.

[13] D.-N. Nguyen, J. Bohata, M. Komanec, S. Zvanovec, B. Ortega, and Z. Ghassemlooy, "Seamless 25 GHz transmission of LTE 4/16/64-QAM signals over hybrid SMF/FSO and wireless link," *J. Lightwave Technol.*, vol. 37, no. 24, pp. 6040–6047, 2019.

[14] R. Van Der Linden, N. C. Tran, E. Tangdiongga, and T. Koonen, "Optimization of flexible non-uniform multilevel PAM for maximizing the aggregated capacity in PON deployments," *J. Lightwave Technol.*, vol. 36, no. 12, pp. 2328–2336, 2018.

[15] K. Matsuda and N. Suzuki, "Hardware-efficient signal processing technologies for coherent PON systems," *J. Lightwave Technol.*, vol. 37, no. 6, pp. 1614–1620, 2019.

[16] "5G spectrum GSMA public policy position," 2018. [Online]. Available: https://www.gsma.com/.

[17] S. Rommel *et al.*, "Outdoor W-Band hybrid photonic wireless link based on an optical SFP+ module," *IEEE Photonics Technol. Lett.*, vol. 28, no. 21, pp. 2303–2306, 2016.

[18] "Universal Mobile Telecommunications System (UMTS); LTE; Active Antenna System (AAS) Base Station (BS) conformance testing; Part 1: conducted conformance testing (3GPP TS 37.145-1 version 14.1.0 Release 14)," 2017.